Journal of Applied Engineering Mathematics

Volume 10, December 2023

Analytical Modeling of Microchannel Temperatures in Thermal Gradient Gas Chromatography Columns

Muhammad Taha, Brandon Page, Jefferson Santos Da Silva

Mechanical Engineering Department
Brigham Young University
Provo, Utah 84602
tahabyu@student.byu.edu, pageb119@byu.edu, bartolomeujeba@gmail.com

Abstract

Thermal Gradient Gas Chromatography (TGGC) is recognized as a pivotal separation technique in the advancement of contemporary chemical research. An inherent challenge in the application of TGGC lies in the precise modeling and control of column temperature, along with the determination of optimal microchannel spacings on the column. This paper aims to report the outcomes of an analytical model devised to evaluate the temperature distribution and spacings for microchannels employed in gas chromatography, specifically focusing on microchannels enveloping a cylindrical column. This paper also discusses the temperature variation along the length of the column for four different separation distances for specific boundary conditions.

Methodology

An analytical model for different boundary conditions is developed and resulting profiles are compared for multiple cases. The setup incorporated a solid cold cylinder to maintain a constant surface temperature at the top side of the vertical column, and a hollow cylinder equipped with cartridge heaters to establish a constant heat flux boundary condition at the bottom side.[6, 1] Given that the heated air could only ascend due to a reduction in density and had no other exit, the cylinder was assumed to be insulated internally.

Analytical Modeling

The comprehensive modeling of the setup posed a complex challenge, necessitating its division into three distinct regions for the sake of simplification. The column was segmented along its length into these regions. The first region is characterized by a constant heat flux boundary condition at the inner surface of the cylinder and insulation on the outer surface.[4] The second region is insulated both inside and outside the cylinder. The third region maintains a constant surface temperature on the inside and an insulated boundary condition on the outer surface. This divisional approach facilitated a more manageable and efficient modeling process. The corresponding geometry and 3D model is illustrated in Figure 1 and Figure 2.

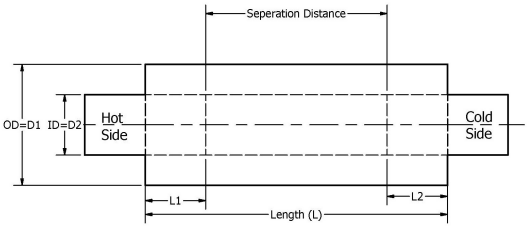

Figure 1: Geometry of the column

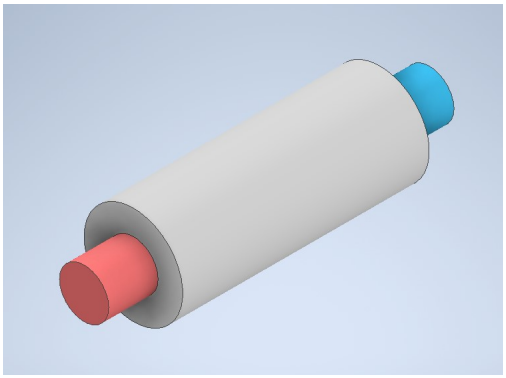

Figure 2: Geometry of the column

The external surface of the setup is assumed to be fully insulated. Given the hollow nature of the cylinder, the assumption of insulation on the inside might initially appear to be an overreach. However, in practical applications, the column would be oriented vertically along its length, with the cold solid side positioned at the top and the hot hollow side at the bottom. The heated air ascends due to the density differences induced by temperature variations. However, the upward movement of the air is impeded by the solid part at the top of the cylinder, preventing its escape. Consequently, it is reasonable to assume that the internal portion of the cylindrical column, which is not in contact with either the hot or cold cylinder, is insulated. This assumption aids in the simplification and accuracy of the modeling process.[5]

Constant Heat Flux Section

In the model, all lengths were rendered dimensionless by the length of the boundary exhibiting constant heat flux. This approach was adopted to facilitate the variation of length for the same model without necessitating multiple alterations of the length. The boundary conditions for the model are illustrated in Figure 3.

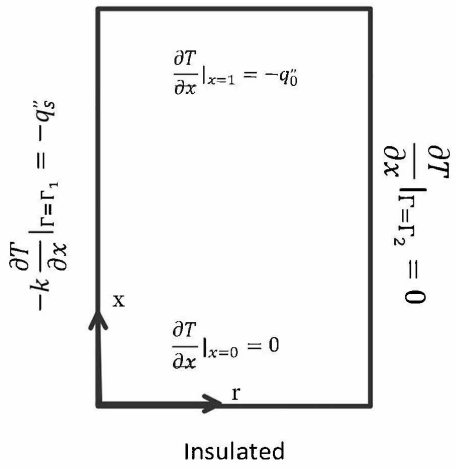

Figure 3: Front view of bottom right corner of the vertical column (Constant heat flux section)

The setup is presumed to exhibit symmetry around its central axis. The boundary conditions are non- homogeneous for the resulting homogeneous partial differential equation (PDE), as shown in equation 1. Both the radial and axial directions are normalized by the length L of the segment. Consequently, the variable r is substituted with the variable Γ and the variable z is substituted with x after normalization. This normalization process simplifies the model.

$$\frac{1}{r}\frac{\partial}{\partial r}\left(r\frac{\partial T}{\partial r}\right) + \frac{\partial^2 T}{\partial z^2} = 0 \tag{1}$$

The solution to the partial differential equation (PDE) (1) is provided below. This solution is derived by solving two scenarios, each with a non-homogeneous boundary condition, and subsequently employing superposition principle to obtain the overall result as shown in Figure 4.

Analytical modelling for heat flux side of the setup Non-dimensionalizing: $x = \frac{z}{L}$; $\Gamma = \frac{r}{L}$

$$\frac{1}{r}\frac{\partial}{\partial r}\left(r\frac{\partial T}{\partial r}\right)+\frac{\partial^2 T}{\partial x^2}=0 \rightarrow \frac{1}{\Gamma}\frac{\partial}{\partial \Gamma}\left(\Gamma\frac{\partial T}{\partial \Gamma}\right)+\frac{\partial^2 T}{\partial x^2}=0$$

Energy Balance: Heat in = Heat out

$$-k\frac{1}{L_1}\frac{\partial T}{\partial x}=\frac{q_s'' D_1 L_1}{(R_2^2-R_1^2)} \rightarrow \ldots$$
$$\left.\frac{\partial T}{\partial x}\right|_{x=1}=-\frac{q'' D_1 L_1^2}{k\left(R_2^L-R_1^L\right)}=-q_0''$$

$$-k\frac{\partial T}{\partial r}=-k\frac{1}{L}\left.\frac{\partial T}{\partial \Gamma}\right|_{\Gamma_1}=\ldots$$
$$q_s'' \rightarrow \left.\frac{\partial T}{\partial \Gamma}\right|_{\Gamma_1}=-\frac{q_s'' L_1}{k}=-q''$$

Note: $x = 1$ represents the boundary in the hot region and center region; (L_1)

A

$$T_A = R(\Gamma)X(x): \quad X'(0)=0; \quad X(1)=0$$

Make a SLP in X:

$$\frac{1}{R}\left(R''+\frac{R'}{\Gamma}\right)=-\frac{X''}{X}=+\lambda^2\Bigg\} X''+\lambda^2 X=0$$

Which has a characteristic equation of

$$c_1\sin(\lambda x)+c_2\cos(\lambda x)$$

$$X'=c_1\lambda\cos(\lambda x)-c_2\lambda\sin(\lambda x)\}\, X'(0)=0,\ c_1=0$$
$$X(1)=0=\cos(\lambda)\rightarrow\lambda=(2n-1)\frac{\pi}{2}$$
$$X=c_2\cos(\lambda x)\Rightarrow\lambda=(2n-1)\frac{\pi}{2};\ n=1,2,3,\ldots$$

$$R''+\frac{R'}{\Gamma}-\lambda^2 R=0\Rightarrow R(\Gamma)=c_3\Gamma_0(\lambda\Gamma)+\ldots$$
$$c_4 k_0(\lambda\Gamma)$$

$$R'=c_3\lambda\Gamma_1(\lambda\Gamma)-c_4\lambda k_1(\lambda\Gamma)|\, R'(\Gamma_2)=0\Rightarrow\ldots$$
$$c_3=c_4\frac{k_1(\lambda\Gamma_2)}{\Gamma_1(\lambda\Gamma_2)}$$

$$R(\Gamma)=c_4\frac{k_1(\lambda\Gamma_2)}{\Gamma_1(\lambda\Gamma_2)}\Gamma_0(\lambda\Gamma)+c_4 k_0(\lambda\Gamma)\rightarrow\ldots$$
$$c_4'\left[k_1(\lambda\Gamma_2)\Gamma_0(\lambda\Gamma)+k_0(\lambda\Gamma)\Gamma_1(\lambda\Gamma_2)\right]$$

$$T_A=R(\Gamma)X(x)=\sum c_n\left[k_1(\lambda\Gamma_2)\Gamma_0(\lambda\Gamma)+\ldots\right.$$
$$\left.k_0(\lambda\Gamma)\Gamma_1(\lambda\Gamma_2)\right]\cos(\lambda x)$$

$$\left.\frac{\partial T_A}{\partial\Gamma}\right|_{\Gamma_1}=-\frac{q_s'' L_1}{k}=\sum_n c_n\left[\lambda k_1(\lambda\Gamma_2)\Gamma_1(\lambda\Gamma_1)+\right.$$
$$\left.\ldots\lambda k_1(\lambda\Gamma_1)\Gamma_1(\lambda\Gamma_2)\right]\cos(\lambda x)$$

$$c_n=\frac{-\frac{q_s'' L_1}{k}\int_0^1\cos(\lambda x)}{B\int_0^1\cos^2(\lambda x)}$$

$$\frac{\partial T_A}{\partial x_1}=-\sum c_n\left[k_1(\lambda\Gamma_2)\Gamma_0(\lambda\Gamma)+\ldots\right.$$
$$\left.k_0(\lambda\Gamma)\Gamma_1(\lambda\Gamma_2)\right]\lambda\sin x$$

$$T=T_A+T_1$$

(B)

$$\frac{1}{R}\left(R''+\frac{R'}{\Gamma}\right)=-\frac{X''}{X}=-\lambda^2\ \text{(Make separable)}$$

$$R''+\frac{R'}{\Gamma}+\lambda^2 R=0 \qquad X''-\lambda^2 X \qquad =0$$

$$R(\Gamma)=c_1 J_0(\lambda\Gamma)+c_2 Y_0(\lambda\Gamma)\}\ ②: R'(\Gamma_1)=0$$
$$R(\Gamma)=-c_1\lambda J_1(\lambda\Gamma)-c_2\lambda Y_1(\lambda\Gamma)\}\ ①: R'(\Gamma_2)=0$$

$$②: c_1=-c_2\frac{Y_1(\lambda\Gamma_2)}{J_1(\lambda\Gamma_2)}\rightarrow\ldots$$
$$①: c_2\frac{Y_1(\lambda\Gamma_2)}{J_1(\lambda\Gamma_2)}J_1(\lambda\Gamma_1)-c_2 Y_1(\lambda\Gamma_1)=0$$

Rearranging: $Y_1(\lambda\Gamma_2)J_1(\lambda\Gamma_1) - J_1(\lambda\Gamma_2)Y_1(\lambda\Gamma_1) = 0$

$$R(\Gamma) = -c_2\frac{Y_1(\lambda\Gamma_2)}{J_1(\lambda\Gamma_2)}J_0(\lambda\Gamma) + \ldots$$
$$c_2Y_0(\lambda\Gamma) = c_2'\left[Y_1(\lambda\Gamma_2)J_0(\lambda\Gamma) - \ldots\right.$$
$$\left.J_1(\lambda\Gamma_2)Y_0(\lambda\Gamma)\right]$$

Solving for x:

$$X(x) = c_1\cosh(\lambda x) + c_2\sinh(\lambda x)$$
$$X'(x) = -c_1\lambda\sinh(\lambda x) + c_2\lambda\cosh(\lambda x)$$

$$③\ X'(0) = 0$$

$$-c_1\lambda\cancelto{0}{\sinh(0)} + c_2\lambda\cancelto{1}{\cosh(0)} = 0 \Rightarrow c_2 = 0$$

$$X(x) = c_1\cosh(\lambda x)$$

$$T_B(\Gamma,\ x) = \sum_n\left[Y_1(\lambda\Gamma_2)J_0(\lambda\Gamma) - \ldots\right.$$
$$\left.J_1(\lambda\Gamma_2)Y_0(\lambda\Gamma)\right]\cosh(\lambda x)$$

$$④\ \left.\frac{dT}{dx}\right|_L = q_0 \rightarrow -k\left[\left.\frac{dT_A}{dx}\right|_L + \ldots\right.$$
$$\left.\left.\frac{dT_B}{dx}\right|_L\right] \rightarrow -q_0 - \left.\frac{dT_A}{dx}\right|_L = \frac{dT_B}{dx}$$

$$\left.\frac{dT_B}{dx}\right|_1 = \sum_n c_nB(-\lambda\sinh(\lambda)) = \left[-q_0 - \frac{dT_A}{dx}\right]$$

$$q_0 = \frac{q_sD_1L_1^2}{k(R_2^2 - R_1^2)}$$

$$c_n = \frac{-\int_{\Gamma_2}^{\Gamma_2}\Gamma A(\Gamma)B(\Gamma)\,d\Gamma}{\lambda\sinh(\lambda)\int_{\Gamma_2}^{\Gamma_2}\Gamma B(\Gamma)^2\,d\Gamma}$$

The equation yields modified Bessel functions[3] as the solution in the radial direction and a cosine function in the axial direction when homogeneity is assumed in the axial direction, as depicted in equation 2. When the boundary conditions are homogeneous in the radial direction, the constant λ is determined such that the resulting solution is an ordinary Bessel function in the radial direction and a hyperbolic cosine function in the axial direction, as illustrated in equation 3. This approach is adopted to leverage the periodicity and orthogonality of Bessel functions to determine the constant in the equation using the non-homogeneous boundary condition.

$$T_A = \sum_n c_n\left(k_1(\lambda_n\Gamma_2)I_0(\lambda_n\Gamma) + \right.$$
$$\left.I_1(\lambda_n\Gamma_2)k_0(\lambda_n\Gamma)\cos(\lambda x)\right. \quad (2)$$

$$T_B = \sum_n c_n\left(Y_1(\lambda_n\Gamma_2)J_0(\lambda_n\Gamma) + \right.$$
$$\left.J_1(\lambda_n\Gamma_2)Y_0(\lambda_n\Gamma)\cosh(\lambda x)\right. \quad (3)$$

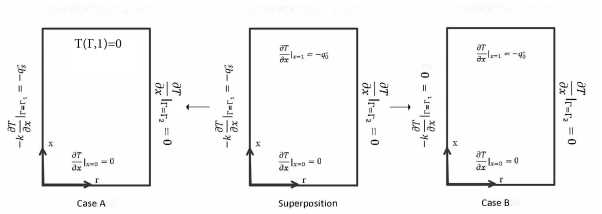

Figure 4: Superposition Principle

Middle Segment of the Column

The segment of the column that is situated in the middle and is not in contact with either the cold or hot side is assumed to be insulated both externally and internally. Given that energy is coming in from the hot side and exiting from the cold side, an energy balance can be applied, as demonstrated in equation 4.

By employing this energy balance, we can determine the flux at the boundary between the hot and middle sections. Under steady-state conditions, we can assume that there is no variation of flux in the radial direction, leading to a linear temperature profile in the axial direction. The temperature gradient of this profile remains constant which is equivalent to the gradient determined from equation 4. Consequently, it can be inferred that the gradient at the boundary between the middle and cold sections will be identical, owing to the linear temperature profile. It should be noted that all aspects of this analysis are predicated on the assumption of constant material properties.

$$2q_s\pi R_1 L_1 = q_0\pi\left(R_2^2 - R_1^2\right) \tag{4}$$

Where q_s is the flux at the hot side, q_0 is the flux at the boundary of hot side and the middle section, R_1 is the internal radius and R_2 is the external radius, and L_1 is the length of the hot section.

Constant Surface Temperature Section

The cold side of the column was modeled with boundary conditions as depicted in Figure 5.

$$\frac{1}{\Gamma}\frac{\partial}{\partial\Gamma}\left(\Gamma\frac{\partial T}{\partial\Gamma}\right) + \frac{\partial^2 T}{\partial x^2} = 0$$

$$\theta = T - T_c \Rightarrow \partial\theta = \partial T$$

$$\frac{1}{\Gamma}\frac{\partial}{\partial\Gamma}\left(\Gamma\frac{\partial\theta}{\partial\Gamma}\right) + \frac{\partial^2\theta}{\partial x^2} = 0$$

$$\begin{aligned}
&① \ \theta\left(\Gamma_1,\ x\right) = 0\\
&② \ \left.\frac{\partial\theta}{\partial\Gamma}\right|_{\Gamma_2} = 0\\
&③ \ \left.\frac{\partial\theta}{\partial x}\right|_{0} = 0\\
&④ \ \left.\frac{\partial\theta}{\partial\Gamma}\right|_{1} = -q_0''
\end{aligned}$$

$$\theta\left(\Gamma_1,\ x\right) = R\left(\Gamma(\ X\left(x\right)\right.$$

$$\begin{aligned}
&① \ R\left(\Gamma_1\right) = 0 \qquad ② \ R'\left(\Gamma_2\right) = 0\\
&③ \ X'\left(0\right) = 0 \qquad ④ \text{ Use to find } C_n
\end{aligned}$$

$$R' = -c_1\lambda J_1\left(\lambda\Gamma\right) - c_2\lambda Y_1\left(\lambda\Gamma\right)$$

$$② \ c_1 = -c_2\frac{Y_1\left(\lambda\Gamma_2\right)}{J_1\left(\lambda\Gamma_2\right)}$$

$$-c_2\frac{Y_1\left(\lambda\Gamma_2\right)}{J_1\left(\lambda\Gamma_2\right)}J_0\left(\lambda\Gamma_1\right) + c_2 Y_0\left(\lambda\Gamma_1\right) = 0$$

Find roots for λ

$$X\left(x\right) = c_3\sinh\left(\lambda x\right) + c_4\cosh\left(\lambda x\right)\} \ ③ \ c_3 = 0$$

$$X'\left(x\right) = c_3\lambda\cosh\left(\lambda x\right) + \ldots$$
$$c_4\lambda\sinh\left(\lambda x\right)\} \ X\left(x\right) = c_4\cosh\left(\lambda x\right)$$

$$\theta\left(\Gamma,\ x\right) = \sum_n c_n\left[Y_1\left(\lambda\Gamma_2\right)J_0\left(\lambda\Gamma\right) - \ldots\right.$$
$$\left.J_1\left(\lambda\Gamma_2\right)Y_0\left(\lambda\Gamma\right)\right]\cosh\left(\lambda x\right)$$

$$\left.\frac{dT}{dx}\right|_1 = -q_0''\sum_n c_n\left[Y_1\left(\lambda\Gamma_2\right)J_0\left(\lambda\Gamma\right) - \ldots\right.$$
$$\left.J_1\left(\lambda\Gamma_2\right)Y_0\left(\lambda\Gamma\right)\right]\left(-\lambda\sinh\left(\lambda\right)\right)$$

$$\frac{q_0''\int_{\Gamma_1}^{\Gamma_2}\Gamma B\left(\Gamma\right)d\Gamma}{\lambda\sinh\left(\lambda\right)\int_{\Gamma_1}^{\Gamma_2}\Gamma B^2\left(\Gamma\right)} = c_n$$

A change of variable was implemented to render the constant surface temperature boundary condition homogeneous which allows the elimination of the usage of superposition principle. The governing partial differential equation (PDE) for the cold side is identical to that for the hot side. The solution resulting from the constant surface temperature condition is presented in equation 5.

$$T = \sum_n c_n Y_1\left(\lambda_n\Gamma_2\right)J_0\left(\lambda_n\Gamma\right) -$$
$$J_1\left(\lambda_n\Gamma_2\right)Y_0\left(\lambda_n\Gamma\right)\cosh\left(\lambda x\right) + T_c \tag{5}$$

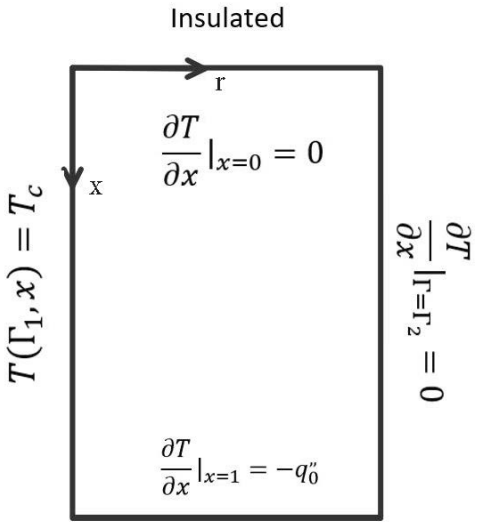

Figure 5: Front view of top right corner of the vertical column (constant surface temperature section)

Results

In a particular scenario with an Outer Diameter (OD) of 4 inches, an Inner Diameter (ID) of 2 inches, and a column length of 10 inches, results were computed and graphically represented for four different separation distances—namely, 2 inches, 4 inches, 6 inches, and 8 inches as shown in Figure 6. The solid hot cylinder maintains a consistent heat flux of 1000 W/m2, and the cold cylinder is set to a constant surface temperature of 25 degrees Celsius, with all other surfaces of the cylinder being insulated. The material is assumed to be copper with a thermal conductivity of 400 W/mK. The temperature at the hot side changes from 25.8 deg C for a 2-inch separation distance to 25 deg C as we go move in length from 0 to 10 inches. The lowest change in temperature is from 25.4 deg c to 25 for an 8-inch separation distance which shows the trend for the temperature difference between cold and hot side, which decreases as we move from a smaller separation distance to a greater one.[2] Figure 7 depicts the graphical representation of these conditions.

Conclusions

This research paper presents an analytical model to study the temperature distribution and spacings of microchannels utilized in Thermal Gradient Gas Chromatography (TGGC) with specific boundary conditions. Four different separation distances were investigated for a specific Outer Diameter, Inner Diameter, and Column length which served as a concrete example to illustrate the impact of separation distances on the temperature distribution. Finally, the results and the effect of separation distance to the temperature profile is discussed.

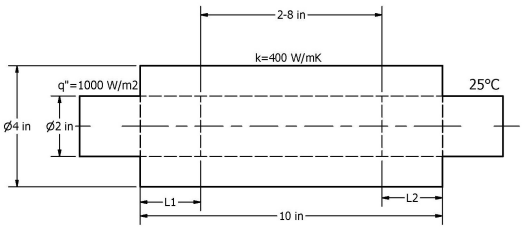

Figure 6: Dimensions for the Specific Case

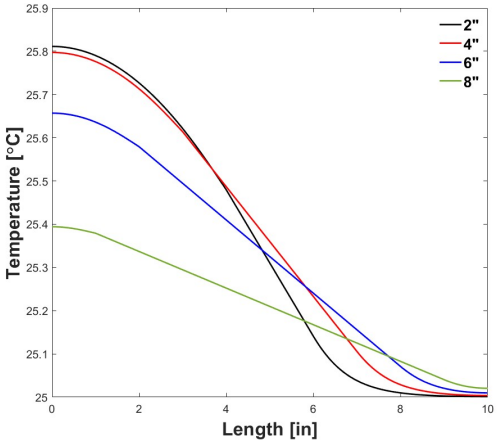

Figure 7: Temperature Profiles for four different Separation Distances

Acknowledgements

References

[1] X. Wang et al. *nalytical modeling of temperature distribution in microchannels for gas chromatography*. Journal of Chromatography A, 2007.

[2] Y. Zhang et al. *Optimal microchannel spacings for efficient gas chromatography*. Analytica Chimica Acta, 2015.

[3] G. B. Arfken and H. J. Weber. *Mathematical Methods for Physicists*. Academic Press, 2001.

[4] Lawrence C. Evans. *Partial Differential Equations*. American Mathematical Society, 2010.

[5] Frank P. Incropera and David P. DeWitt. *Fundamentals of Heat and Mass Transfer*. John Wiley and Sons, 2017.

[6] R. M. Smith and D. S. Richards. *Thermal Gradient Gas Chromatography*. Analytical Chemistry, 1986.

